JOURNAL OF MATERIALS SCIENCE 23 (1988) 194–200

Mechanical behaviour of $[0, \pm 60]_s$ P100/6061 Al composites

V. C. NARDONE, J. R. STRIFE
United Technologies Research Center, E. Hartford, Connecticut 06108, USA

The tensile and compressive behaviour of P100 graphite fibre reinforced 6061 Al in the $[0, \pm 60]_s$ configuration was determined as a function of orientation. The experimentally determined values of the elastic modulus and strength of the composites are compared with those predicted from classical laminate theory. In general, there is good agreement between the predicted and observed values for testing in the longitudinal orientation, but discrepancies exist for testing in the transverse and 45° orientations. A detailed examination of composite failure modes is also presented and discussed.

1. Introduction

Continuous fibre reinforced composites in unidirectional format generally exhibit highly anisotropic properties, with strength and modulus values being much greater parallel to the fibre direction than in the transverse direction. Quasi-isotropic laminates such as the $[0, \pm 60]_s$ configuration can be utilized to create more isotropic composite sheets. It is predicted using classical laminate theory, that for the $[0, \pm 60]_s$ construction, isotropic in-plane elastic properties should result. The current study focuses on an evaluation of high modulus pitch fibre reinforced 6061 Al composites configured in the $[0, \pm 60]_s$ format. Both tensile and compression testing is performed on the composites as a function of orientation within the plane of reinforcement. The strength and modulus values obtained are compared with that predicted by classical laminate theory [1] and the Tsai–Hill failure criteria [2, 3]. In addition, a detailed examination of the failure modes occurring in the composite is presented and discussed.

2. Materials and experimental procedure

Six ply panels with a fibre orientation of $[0, \pm 60]_s$ were consolidated using vacuum diffusion bonding of plies constructed from collimated P100 reinforced liquid metal infiltrated 6061 wires. The P100/6061 wires were supplied by Materials Concepts Inc, Colombus, Ohio, and the panels were consolidated utilizing established procedures by DWA Composite Specialties, Inc, Chatsworth, California. Foils of 6061 aluminium were utilized as ply separators and cladding for the composites. A typical microstructure is shown in Fig. 1. Note the presence of cladding and separator foils in the composite microstructure. The fibre volume fractions of the panels utilized in this study are listed in Table I, as determined by acid dissolution.

Tensile specimens 0.76 cm in width were diamond saw cut from the panels with the intended load axis at 0° (longitudinal), 45°, or 90° (transverse) to the zero degree fibre direction. Fibreglass doublers were adhesive bonded to the specimens creating gauge lengths of 3.8 cm for the longitudinal and transverse specimens, and 2.5 cm for the 45° oriented specimens. Resistance strain gauges were bonded to both sides of the gauge sections for measurement of strain as a function of stress. All specimens were loaded at a constant crosshead deflection rate of 0.0254 cm min^{-1}. The specimens were tested in the as-fabricated condition.

Specimens for compression testing were diamond saw cut from the plates in the longitudinal and transverse orientation. The compression testing conformed to ASTM Designation D3410 with the exception that the specimen thickness of 0.35 cm exceeded the maximum recommended value of 0.30 cm. Steel doublers were bonded to the grip areas creating a nominal gauge length of 1.27 cm. Resistance strain gauges were bonded to both sides of the specimens for measurement of strain. All tests were conducted at a constant crosshead speed of 0.0127 cm min^{-1}. The specimens were tested in the as-fabricated condition.

3. Experimental results

3.1. Tensile test results

The room temperature tensile properties of the $[0, \pm 60]_s$ composite are summarized in Table II, and typical stress–strain curves are shown in Fig. 2. The results show significant anisotropy in stress–strain behaviour as a function of orientation. The elastic modulus averaged 137 GPa in the longitudinal orientation, compared to average values of 107 GPa in the transverse orientation, and 101 GPa at 45° to the longitudinal axis. The strength values were even more anisotropic, with the longitudinal strength averaging 257 MPa while the transverse and 45° strengths averaged 142 and 136 MPa, respectively. In addition, the longitudinal stress–strain behaviour shown in Fig. 2 is much more linear relative to the other orientations.

A comparison of the gauge section failures for all three specimen orientations is shown in Fig. 3. Note that separation is readily apparent within the plies of the transverse samples, as evidenced by a rotation of portions of the plies toward the applied stress axis.

0022–2461/88 $03.00 + .12

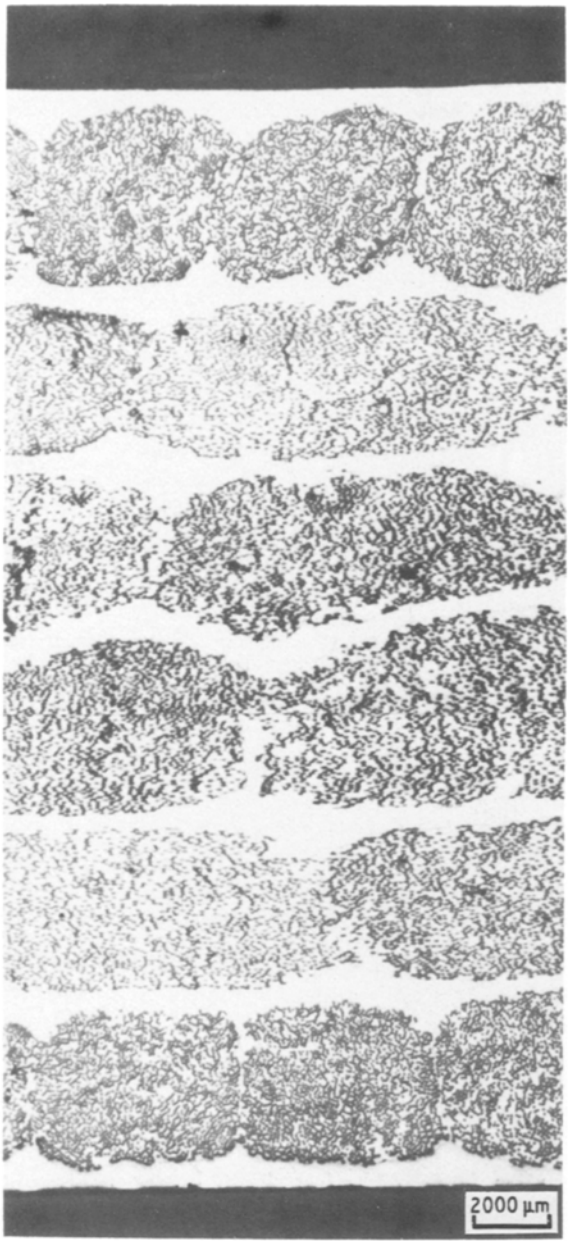

Figure 1 Representative longitudinal cross-section of the $[0, \pm 60]_s$ P100/6061 Al composite.

This intraply separation is evident in both the interior $\pm 30°$ plies and the exterior 90° plies. Evidence of intraply separation and rotation toward the stress axis is also present in the other specimen orientations as reported below.

The fracture surfaces of samples are shown in Figs 4 to 6. For the longitudinal sample, the inner two 60° plies have a macroscopically smooth fracture surface indicative of shear failure or fibre/matrix interface failure. The remaining plies show extensive fibre failure. Intraply separation and rotation to the applied stress axis was evident in the fibre failure mode of the $+60°$ plies. The above pattern was true for five of the six samples tested. In the one exception, a smooth fracture surface was evident for the two outer 60° plies, while fibre breakage occurred on the other four plies. For the transverse sample shown in Fig. 5 the interior two plies have a macroscopically smooth fracture surface, but the other plies show some areas of fibre failure and rotation toward the applied stress axis. This fracture behaviour was evident in all transverse samples tested. The fracture surface of 45° samples is given in Fig. 6. In this case, there is a shear failure of both the inner two plies oriented at 75° and the outer two plies oriented at $-45°$. The remaining two $+15°$ plies exhibit fibre breakage that is similar to that observed for the longitudinal fractures.

TABLE I Volume fraction of P100 fibres in the $[0, \pm 60]_s$ composite panels

Panel	Vol % fibre
5283	36.1
5370	39.4
5371	38.6
5372	40.5

TABLE II Room temperature tensile properties of the $[0, \pm 60]_s$ P100/6061-Al composite*

Panel	E (GPa)	*UTS* (MPa)	εf (%)
	Longitudinal orientation		
5370	130	222	0.19
5370	139	254	0.20
5371	135	244	0.23
5371	136	249	0.24
5372	152	288	0.26
5372	132	286	0.28
Average	137 ± 8	257 ± 23	0.23 ± 0.03
	Transverse orientation		
5370	111	146	0.35
5370	119	159	0.25
5371	106	133	0.21
5371	106	137	0.35
5372	108	142	0.28
5372	92	132	0.35
Average	107 ± 8	142 ± 9	0.30 ± 0.06
	45° orientation		
5283	104	126	0.39
5283	95	145	0.28
5283	103	137	0.28
Average	101 ± 5	136 ± 10	0.32 ± 0.06

*E = Elastic Modulus; UTS = Ultimate Tensile Strength; εf = Failure Strain

TABLE III Room temperature compression properties of the $[0, \pm 60]_s$ P100/6061-Al composite

Panel	E (GPa)	Failure stress (MPa)
	Longitudinal properties	
5370	127	115
5370	128	116
5371	121	110
5371	118	111
5372	126	112
5372	129	116
Average	125 ± 4	114 ± 3
	Transverse properties	
5372	109	104
5372	110	109
5372	105	104
Average	108 ± 3	106 ± 3

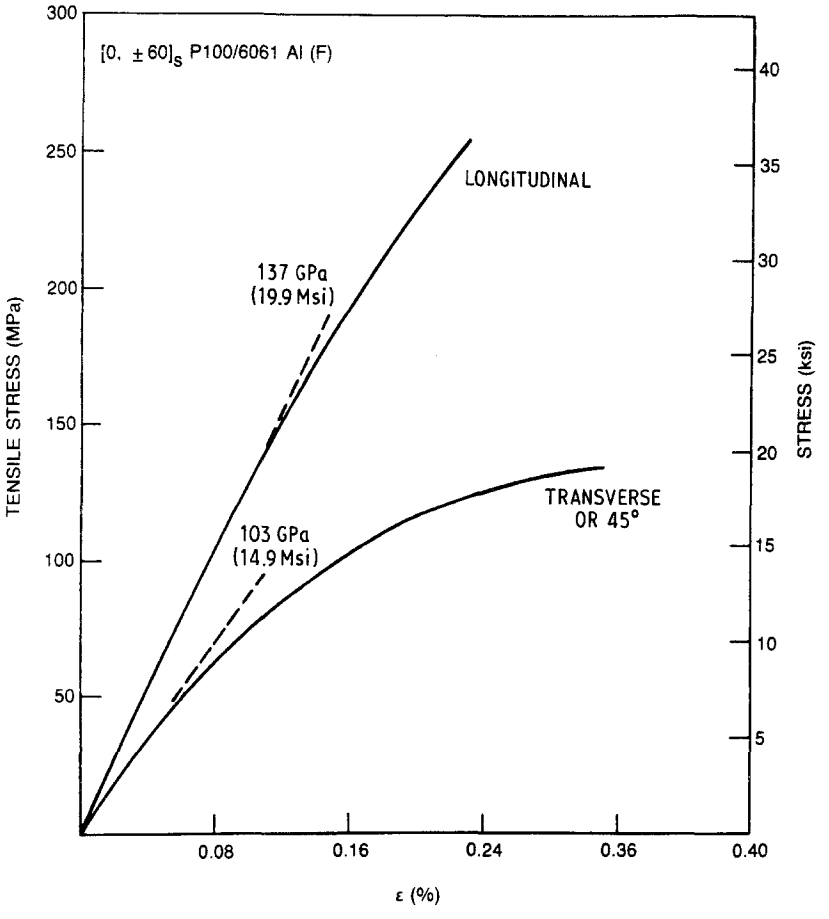

Figure 2 Tensile stress–strain behaviour of the $[0, \pm 60]_s$ P100/6061 Al(F) composite. Msi = 10^6 p.s.i., ksi = 10^3 p.s.i.

3.2. Compression testing

The room temperature compression properties are summarized in Table III, and compression stress–strain curves are shown in Fig. 7. In contrast to the tensile results, the compression data is more quasi-isotropic. The average strength and modulus in the longitudinal direction are 114 MPa and 125 GPa, respectively, compared with average values of 106 MPa and 108 GPa in the transverse direction. Fig. 7 indicates, however, that the longitudinal stress–strain behaviour is much more linear than the transverse case.

Despite the similarity of the strength values displayed in the longitudinal and transverse directions, two distinctly different failure modes occurred as a function of orientation. Failure occurred in the longitudinal samples where there was a slight buckling of one of the outer piles oriented at 0°. There was a lack of any

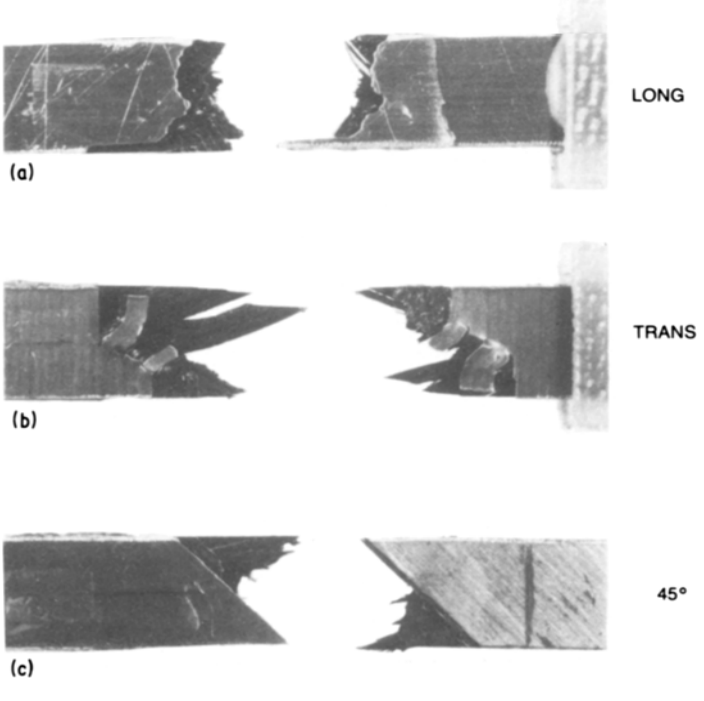

Figure 3 Gauge section tensile failures for all three $[0, \pm 60]_s$ P100/6061 Al specimen orientations. (a) Long, (b) trans, (c) 45°.

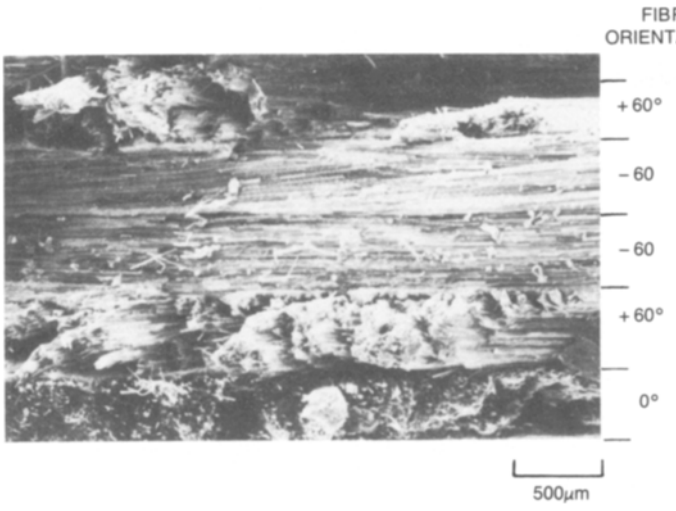

Figure 4 Tensile fracture surface of the $[0, \pm 60]_s$ P100/6061 Al composite in the longitudinal orientation.

apparent damage in the inner plies. In the case of the transverse specimens, cracking between the interior plies oriented at $-30°$ and the adjacent $+30°$ plies was readily apparent as shown in Fig. 8.

4. Discussion

4.1. Tensile modulus and strength

A comparison of the predicted and measured tensile properties of the $[0, \pm 60]_s$ composite is presented in Table IV. Predictions were made using experimentally determined values for Poisson's ratio (0.27), the longitudinal modulus (333 GPa) and strength (745 MPa), as well as the transverse modulus (29 GPa) and strength (21 MPa) for a 40 vol % P100 reinforced 6061 Al unidirectional composite as reported in [4]. The values used for the shear modulus (17 MPa) and (31 MPa) strength are also the same as those used in [4].

The results presented in Table IV for the tensile modulus indicate that the longitudinal test results agree very well with that predicted from classical laminate theory, while modulus values for the other two orientations are substantially less than predicted. The reason for the discrepancy may be due to the method in which strain was measured in the samples. Specifically, strain gauges were bonded to the outer fibre plies. For the longitudinal samples the outer fibre plies were oriented at 0° to the applied load, while in the transverse samples the angle was 90° and in the 45° samples the angle was 45°. The stiffness of a ply is a very strong function of the angle between the applied load and the fibre axis, being much greater for small angles. Thus, the stiffness of the longitudinal samples wil be primarily controlled by the outer 0° plies, while the stiffness of the transverse and 45° samples will be primarily controlled by the inner 30° plies and 15° plies, respectively. The large difference in stiffness among the plies in a given sample may result in a non-constant strain profile being present in the through thickness direction of the composite. Strain will be less in the stiffer plies for any given value of the applied load. Since strain is being measured from gauges attached to low stiffness outer plies in both the transverse and 45° samples, a somewhat low value for the measured modulus may result.

The strength values for the $[0, \pm 60]_s$ composite were calculated using the Tsai–Hill failure criteria [2–3]. Specifically, the failure stress associated with each of the individual plies was determined. For the longitudinal orientation, the 60° plies are predicted to fail at a load of 119 MPa. Assuming that the interior plies fail at 119 MPa, the composite then behaves as a 0° unidirectional material since the outer 0° plies can sustain the applied load. The estimated composite failure stress may then be simply calculated by multiplying the 0° unidirectional failure stress (745 MPa) by 1/3 since these plies occupy one third of the composite cross-section. The result is an estimated strength of 248 MPa, which is in excellent agreement

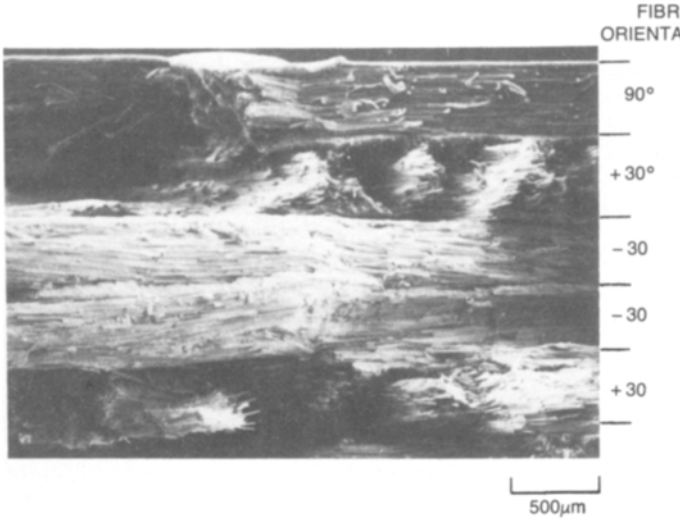

Figure 5 Tensile fracture surface of the $[0, \pm 60]_s$ P100/6061 Al composite in the transverse orientation.

TABLE IV Comparison of predicted and measured $[0, \pm 60]_s$ tensile properties

	Experimentally measured	Predicted*
Longitudinal		
Modulus (GPa)	137	134
Strength (MPa)	257	248
Transverse		
Modulus (GPa)	107	134
Strength (MPa)	142	105
45°		
Modulus (GPa)	101	134
Strength (MPa)	136	108

*Tsai–Hill failure criteria (see text).

with the average measured value of 257 MPa. The near linear tensile stress–strain behaviour reported in Fig. 2 for the longitudinal orientation is further confirmation that strength is controlled by the outer 0° plies.

For the transverse orientation, the Tsai–Hill failure criteria predicts that the outer 90° plies will fail first at an applied load of 105 MPa. Once this occurs, the composite will behave as a $[\pm 30]_s$ configuration, which has a predicted Tsai–Hill failure stress of 111 MPa. The $[\pm 30]_s$ failure stress of 111 MPa must be multiplied by 2/3 since these plies occupy two thirds of the composite cross-section. The predicted failure stress of 74 MPa is less than the failure stress of the 90° plies, so that failure of the 90° plies causes immediate composite failure. Thus, the predicted failure stress for the transverse orientation is 105 MPa, which is somewhat less than the observed value of 142 MPa.

The first ply failure in the 45° specimen orientation is predicted to occur in the +75 plies at a stress of 108 MPa. Once this takes place, the composite will behave as if it possessed a $[-45, +15]_s$ configuration. The Tsai–Hill failure stress for a $[-45, +15]_s$ composite is 145 MPa, with its strength being controlled by failure of the 45° plies. Taking this value and multiplying by 2/3 (the −45, +15 areal fraction) results in a composite failure stress of 87 MPa. Thus, composite failure should occur immediately after the failure of the 75° plies at 108 MPa, which is somewhat less than the observed value of 136 MPa.

The fact that the Tsai–Hill failure criteria tends to underestimate the strength of angle-plied composites containing separator foils has been previously reported [4]. During shear failure of a given ply that has an adjacent ply oriented in a different direction, the interface between the fibre ply and separator foil must also fail. The added stress necessary to fail the fibre ply/separator foil interface is not considered in the Tsai–Hill failure criteria. Thus, for the transverse and 45° specimen orientations where shear failure effects composite strength, the predicted strength values are less than experimentally observed. The importance of the presence of the separator foils in composite failure is confirmed in the failure mode analysis presented below.

TABLE V Summary of tensile failure mode observations in the $[0, \pm 60]_s$ composites

Ply orientations (degree)	Observed ply failure modes
Longitudinal sample	
0	Fibre failure
+60	Fibre failure*
−60	Shear failure
−60	Shear failure
+60	Fibre failure*
0	Fibre failure
Transverse sample	
90	Fibre/matrix interface failure*
+30	Fibre failure*
−30	Shear failure*
−30	Shear failure*
+30	Fibre failure*
90	Fibre/matrix interface failure*
45° sample	
−45	Shear failure
+15	Fibre failure*
+75	Shear failure
+75	Shear failure
+15	Fibre failure*
−45	Shear failure

*Intraply separation and rotation also present.

4.2. Tensile failure modes

A summary of the observed tensile failure modes in the $[0, \pm 60]_s$ composite is presented in Table V. It is noted that in five of the six longitudinally oriented samples tested, shear failure occurred on the inner

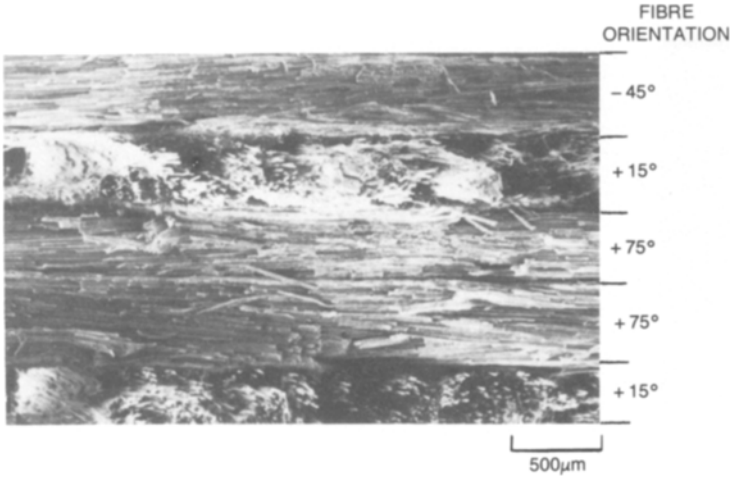

Figure 6 Tensile fracture surface of the $[0, \pm 60]_s$ P100/6061 Al composite in the 45° orientation.

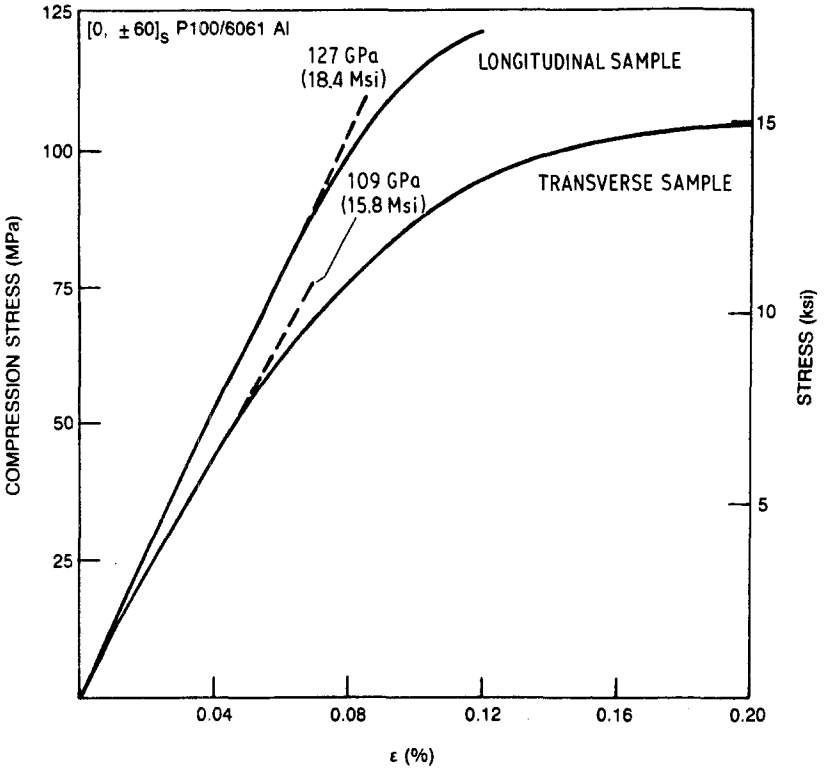

Figure 7 Compression stress–strain behaviour for the [0, ±60]$_s$ P100/6061 Al composites. Msi = 10^6 p.s.i., ksi = 10^3 p.s.i.

−60° plies while fibre failure occurred in the outer +60° plies. This fibre failure is accompanied by rotation to the applied stress axis in the +60° plies.

The preferential shearing of the inner −60° plies is not due to a larger resolved shear stress, as the calculated shear stress is the same for both the −60° and +60° plies. However, as described in detail elsewhere [4], and mentioned above, the presence of interply separator foils introduces a barrier to the shear process in multiaxially reinforced composites. Specifically, in order for a given ply to shear, it must fail the interface between itself and the separator foil when the adjacent ply is oriented in a different direction. If the inner −60° plies shear together, only two areas of fibre ply/separator foil interface must fail. These are the areas between the −60° and +60° plies. If, however, the outer +60° plies were to fail in shear, a total of four areas of fibre/ply separator foil interfaces must fail. The two interfaces between the +60° and −60° plies, and the two interfaces between the +60° and 0° plies. This results in the preferential shearing of the inner −60° plies.

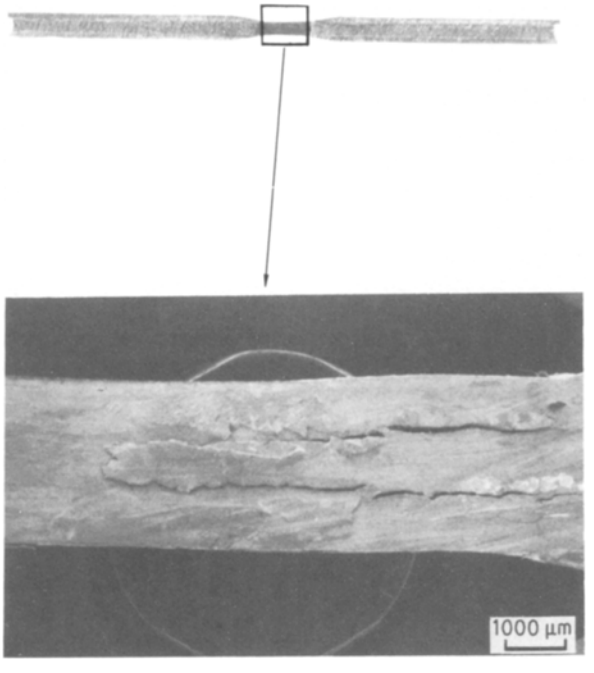

Figure 8 Failed [0, ±60]$_s$ P100/6061 Al transverse compression specimen as viewed from the side.

Once the −60° plies shear and the specimen begins to separate, a state of stress is imposed on the nonshearing +60° plies that acts both perpendicular to the fibre direction and parallel to the load direction. The net result is a rotation of the nonshearing plies toward the applied stress axis and accompanying fibre failure. This biaxial state of stress can account for fibre failure being present in plies oriented at large angles relative to the applied stress.

The preferential shearing of the inner two plies and fibre failure for plies oriented at large angles relative to the applied stress is also apparent for the transverse and 45° specimen orientations as summarized in Table V. The preferential shearing of the −30° plies in the transverse samples and +75° plies in the 45° samples may once again be attributed to the influence of separator foils as described above. Fibre failure being present in plies oriented at large angles relative to the applied stress may again be attributed to the stress state imposed by the shearing of differently oriented plies.

An additional observation is the evidence of intraply separation in the −30° plies of the transverse sample that failed in shear. This separation may be attributed to presence of the separator foils restricting the shear process, and in turn imposing a stress state that acts perpendicular to the fibre direction. The reason for the intraply separation being absent in the sheared −60° plies of the longitudinal sample and

TABLE VI Comparison of predicted and measured $[0, \pm 60]_s$ compression properties

	Experimentally measured	Predicted*
Longitudinal		
Modulus (GPa)	125	125
Strength (MPa)	114	120
Transverse		
Modulus (GPa)	108	125
Strength (MPa)	106	99

*Tsai–Hill criteria (see text).

$+75°$ plies of the transverse sample is due to the larger angle of these sheared plies.

4.3. Compression testing results

A comparison of the predicted and measured compression properties for the $[0, \pm 60]_s$ composites is given in Table VI. The same values used to predict the composite tensile properties were assumed in calculating the composite compressive properties with the following exceptions: the longitudinal strength value for a 0° unidirectional sample was taken as 359 MPa [5] and the longitudinal modulus was taken as 304 GPa [5].

As was the case with the tensile moduli, the experimentally determined longitudinal compressive modulus agrees very well with the predicted value, while the transverse modulus is less than predicted. The same explanation used to account for the tensile moduli would apply here. Since the outer plies where strain is being monitored in the transverse samples are much more compliant than the interior plies, a somewhat low value for the elastic modulus is measured assuming that a non-constant strain profile is present in the through thickness direction of the composite.

The predicted compression strength of the composites was determined using the Tsai–Hill failure criteria. For the longitudinal orientation, it is predicted that first ply failure occurs in the $\pm 60°$ plies at a stress of 110 MPa. Once this occurs, the composite will behave as a 0° undirectional sample that has a compressive failure stress of 359 MPa [5]. Multiplying this value by 1/3 (the 0° ply areal fraction) gives a predicted composite failure stress of 120 MPa. Thus, compression strength should be controlled by failure of the outer 0° plies as was the case with the tensile testing. The agreement between the predicted (120 MPa) and experimentally observed value (114 MPa) is very good. Strength being controlled by the outer 0° plies is also indicated by the near linear stress–strain behaviour of the longitudinal sample reported in Fig. 7.

The first ply failure of the transverse orientation is predicted to occur in the 90° plies at a stress of 99 MPa. The predicted compressive failure stress for the remaining $[\pm 30]_s$ plies is 106 MPa, or an estimated composite failure stress 71 MPa. Thus, failure of the composite should result from failure of the outer 90° plies at a stress level of 99 MPa, which agrees well with the measured value of 106 MPa.

The failure modes of the compression samples were distinctly different. The longitudinal samples showed no damage in the interior plies, and the outer plies showed only a slight buckling. In contrast, the transverse samples showed interior ply cracking (see Fig. 8) that resulted from the shear failure of the plies. The failure modes tend to suggest that the longitudinal strength is controlled by failure of the outer plies while the transverse sample failure involves shearing of the interior $\pm 30°$ plies.

5. Conclusions

Classical laminate theory accurately predicts the tensile and compressive longitudinal modulus of the $[0, \pm 60]_s$ composite but overestimates the modulus values for other orientations. The discrepancy may be due to strain being measured with gauges mounted on the compliant outer fibre plies in the transverse and 45° specimen orientations.

The longitudinal tensile strength of the composite is controlled by failure of the outer fibre plies, while the strength in other orientations is controlled by first ply failure in the composite. The Tsai–Hill failure criteria accurately predicts longitudinal strength, but underestimates strength in the transverse and 45° orientations.

The longitudinal compression strength of the $[0, \pm 60]_s$ composite is controlled by the outer fibre plies, while failure of the 90° plies control strength in the transverse orientation. Failure modes and stress–strain behaviour also indicate that strength is controlled by the outer fibre plies. The Tsai–Hill failure criteria accurately predicts the composite compressive strength.

Tensile failure in all specimen orientations show preferentially shearing of the interior fibre plies. This may be attributed to the influence of the separator foils in shearing of multiaxially reinforced composites.

Fibre failure can occur in $[0, \pm 60]_s$ composites even when the angle between the stress axis and the fibre orientation is large. This fibre failure is due to a resolved biaxial stress state acting on a ply when an adjacent ply begins to shear.

Acknowledgement

The support of the Air Force Wright Aeronautical Laboratories under Contract F33615-81-C-5128 in performing this research is gratefully acknowledged.

References

1. J. C. HALPIN, "Primer on Composite Materials: Analysis" (Technical Publication Co., Lancaster, Pennsylvania, 1984).
2. S. W. TSAI, in "Fundamental Aspects of Fibre Reinforced Plastic Composites", edited by R. T. Schwartz and H. S. Schwartz (Interscience, New York, 1968) Vol. 3, p.3.
3. *Idem*, "Strength Characteristics of Composite Materials", NASA CR-224 (1965).
4. V. C. NARDONE and J. R. STRIFE, *J. Mater. Sci.* **22** (1987) pp. 592–600.
5. *Idem*, unpublished research, 1986.

Received 17 February
and accepted 28 April 1987